On the Use of AM1 and MNDO Wave Functions to Compute Accurate Electrostatic Charges

M. Orozco

Departamento de Bioquímica y Fisiología, Facultad de Química, Universidad de Barcelona, C/. Martí i Franqués 1, 08028 Barcelona, Spain

F. J. Luque

Departamento de Farmacia, Unidad de Físico-Química, Facultad de Farmacia, Universidad de Barcelona, Av. Diagonal s/n, 08028 Barcelona, Spain

Received 30 October 1989; accepted 23 March 1990

A new strategy to evaluate accurate electrostatic charges from semiempirical wave functions is reported. The rigorous quantum mechanical molecular electrostatic potentials computed from both MNDO and AM1 wave functions are fitted to the point-charge molecular electrostatic potential to obtain the electrostatic charges. The reliability of this strategy is tested by comparing the semiempirical electrostatic charges for 21 molecules with the semiempirical Mulliken charges and with the ab initio STO-3G and 6-31G* electrostatic charges. The ability of the dipoles derived from the semiempirical electrostatic and Mulliken charges as well as from the SCF charge distributions to reproduce the ab initio 6-31G* electrostatic dipoles and the gas phase experimental values is determined. The statistical analysis clearly point out the goodness of the semiempirical electrostatic charges, specially when the MNDO method is used. The excellent relationships found between the MNDO and 6-31G* electrostatic charges permit to define a scaling factor which allows to accurately reproduce the 6-31G* electrostatic charge distribution as well as the experimental dipoles from the semiempirical electrostatic charges.

INTRODUCTION

Molecular mechanics and dynamic methods are based on the assumption that the energy of a molecule can be determined from a series of classical terms: (1) the bonded energy, which includes stretching, bending, and torsion terms, (2) the van der Waals interactions, and (3) the electrostatic energy. All these terms are expressed by means of very simple equations, where some parameters are determined by fitting to experimental data. This simplicity drastically reduces the computational requirements with respect to quantum mechanical methods, which makes possible the study of the characteristics of macromolecules like nucleic acids or proteins.

Since the electrostatic term has a major relevance in the whole energy of the molecule, the correct representation of such interaction plays a key role in determining reliable results from molecular mechanic and dynamic computations. The electrostatic interaction energy can be rigorously evaluated from quantum chemical calculations at the SCF level[1] and can be approximately expressed by combining "short range" repulsive term and a series of multipole-multipole interaction terms.[2–4] In molecular mechanics and dynamics methods, the "short range" repulsive term is included within the van der Waals energy and the series of multipole-multipole interactions are limited to the monopole-monopole term. Then, the electrostatic energy is expressed according to eq. (1), where ε is the dielectric constant and q_i and q_j are point charges usually centered at the nuclei.

$$E = \sum_{i,j} \frac{q_i q_j}{\varepsilon r_{ij}} \tag{1}$$

The atomic charge is not an exactly defined physical property, which is defined according to several strategies.[5–9] The most widely used procedure is the population analysis proposed by Mulliken,[5] the popularity of this method being due to its simplicity, but the poor performance of Mulliken charges to reproduce the essential features of electrostatic potential maps is well established.[6,10–12] More recently, electrostatic charges obtained by fitting the rigorously defined quantum mechanical and the point-charge electrostatic potentials have been reported.[6] The reliability of electrostatic charges to provide an accurate description of isopotential maps, as well as to reproduce experimental dipole moments and electrostatic interactions between molecules has been discussed.[6,10,11,13,14] The great quality of

Journal of Computational Chemistry, Vol. 11, No. 8, 909–923 (1990)

CCC 0192-8651/90/080909-15$04.00

these charges explain their inclusion in force fields like Kollman's,[15-17] which is largely used for molecular mechanics and dynamics studies of proteins and nucleic acids. However, the applicability of molecular electrostatic potential-derived atomic charges is seriously limited, since their computation present in practice several problems mainly associated to the calculation of the ab initio wave function, which becomes more difficult as the size of the molecule or the quality of the basis set increases.

The computational cost of the ab initio wave function makes interesting the use of other wave functions to calculate reliable molecular electrostatic potentials. In this sense, the employ of semiempirical wave functions has been reported elsewhere.[18-23] Pullman and co-workers discussed the ability of the CNDO[24,25] wave function to reproduce the most relevant features of isopotential maps, but several failures of both CNDO and INDO[26] wave functions to reflect some fine essential details have been pointed out.[20,27-30] Recently, the reliability of the MNDO[31] wave function to provide reliable electrostatic potentials has been explored.[23] The comparative analysis of molecular electrostatic potentials computed from the semiempirical and ab initio wave functions stated that the characteristics of MNDO derived isopotential maps can be related to those determined from the ab initio wave function calculated at the 6-31G*[32] level.

In this article, the electrostatic charges evaluated at a low computational cost by fitting to molecular electrostatic potentials computed from semiempirical wave functions have been examined. Both MNDO and AM1[33] methods have been considered. Electrostatic and Mulliken charges derived from such semiempirical methods have been compared with those obtained from ab initio computations using STO-3G[34] and 6-31G* basis sets. The analysis has been completed by comparing the dipoles derived from electrostatic and Mulliken charges with both ab initio and experimental dipole moments.

METHODS

Quantum chemical molecular electrostatic potential at a point r_1 is defined according eq. (2),[35] where Z_A is the nuclear charge of atom A, located at R_A, and $\rho(r)$ is the molecular electron density. The first term in the right-hand side of eq. (2) reflects the electrostatic repulsion between nuclei and the positive unit charge locate at r_1, whereas the second one corresponds to the attractive electrostatic term generated by the electronic charge distribution extended in the whole of space.

$$V(r_1) = \sum_A \frac{Z_A}{|r_1 - R_A|} - \int \frac{\rho(r)}{|r_1 - r|} dr \qquad (2)$$

Within the framework of the MO-LCAO approximation, eq. (2) can be rewritten in terms of the basis set of atomic orbitals χ, $P_{\mu\nu}$ being the element $\mu\nu$ of the first-order density matrix.

$$V(r_1) = \sum_A \frac{Z_A}{|r_1 - R_A|} - \sum_\mu \sum_\nu P_{\mu\nu} \int \frac{\chi_\mu(r)\chi_\nu(r)}{|r_1 - r|} dr \qquad (3)$$

The characteristics of MNDO and AM1 methods imply certain consequences for computing molecular electrostatic potentials (23)

1. The semiempirical wave function must be deorthogonalized to describe adequately the essential details of isopotential maps.[18,21,30] For this purpose, the eigenvectors C' expressed in the orthogonal basis set are transformed by using Löwdin's inverse transformation (reference 36; eq. 4), where S is the overlap matrix and C represents the deorthogonalized eigenvectors, which are then used to calculate the elements of the density matrix.

$$C = S^{-1/2}C' \qquad (4)$$

2. Each Slater type orbital of the minimal basis set employed in both MNDO and AM1 methods is fitted to four gaussian functions to facilitate the calculation of integrals in eq. (3).
3. Since MNDO and AM1 are all-valence electron methods, the "core" effective charge is used to evaluate the nuclear electrostatic term.

Accordingly, the only differences between molecular electrostatic potentials computed from semiempirical and ab initio wave functions lye in the origin of the first-order density matrix and in the freezing of the inner electrons.

Electrostatic charges were determined following the procedure reported by Singh and Kollman.[14] Thus, electrostatic charges are obtained by fitting the rigorous quantum mechanical and the point-charge electrostatic potential calculated in points placed on a set of layers out of the van der Waals radii of the atoms by means of the Levenberg–Marquardt nonlinear optimization procedure.[37] Charges fitted to electrostatic potentials derived from semiempirical wave functions were compared with those obtained from ab initio calculations at both STO-3G and 6-31G* levels. Dipole moments determined from such point charges as well as those derived from Mulliken population analysis and from the SCF charge

distributions were compared with gas phase experimental values in order to examine in more detail the reliability of electrostatic charges.

The comparative study was carried out according to the following statistical tests: (1) a simple regression analysis where variables x and y are related by means of an equation of the type $y = ax + b$ was performed to evaluate the correlation between variables x and y, the quality of the fitting being determined by Pearson's correlation coefficient (r); (2) a nonconstant regression analysis where variables x and y are related by means of an equation of the type $y = cx$ was done to compute the ratio between values of variables x and y; (3) the root mean square (RMS) deviation defined according eq. (5) was determined to calculate absolute differences between two variables; (4) the relative RMS deviation (eq. (6)) was used to compute the relative deviation between variables x and y. This latter test was exclusively employed to explore the goodness of the fitting between quantum mechanical and point-charge electrostatic potentials.

$$\text{RMS deviation} = \sqrt{\frac{\sum_i (y_i - x_i)^2}{n}} \qquad (5)$$

n is the number of points used for the fitting procedure.

$$\text{Relative RMS deviation} = \sqrt{\frac{\sum_i (y_i - x_i)^2}{\sum_i y_i^2}} \qquad (6)$$

Semiempirical calculations were performed using a locally modified version[38] of MOPAC program[39] from standard parameters.[31,33,40,41] Experimental data for molecular geometries were taken from the literature.[33,42] HONDO-76 program[43] was used in ab initio computations. Molecular electrostatic potentials were evaluated with a locally modified version of the Pisa group program. The layers of points used to evaluate the electrostatic potential were defined following the Connolly's strategy.[44]

RESULTS

Following the strategy suggested by Singh and Kollman,[14] we first determined the dependence of the electrostatic charges on the surface points at which the molecular electrostatic potential derived from the semiempirical wave function is evaluated, since the conclusions established from ab initio calculations could not remain valid when dealing with semiempirical wave functions. Particularly, this study examined the modulation of electrostatic charges for formamide[45] due to (1) the distance between the molecule and the inner layer, i.e., that surface located closest to the molecule, (2) the number of points, and (3) the number of layers.

The effect that the distance from the inner layer to the molecule has on the electrostatic charges and the dipoles for formamide derived from both MNDO and AM1 calculations is reported in Table I. All of these calculations were carried out considering four layers, each one separated 0.2 Å from the another, and 200 points. The inner layer was located at 1.2, 1.4, 1.6, and 1.8 times the van der Waals radii of the atoms. Results displayed in Table I point out a close similarity between charges and dipoles irrespective of the distance from the inner layer to the molecule, specially for a distance equal or greater than 1.4 times the van der Waals radii of the atoms. The relative RMS deviations between quantum mechanical and point-charge electrostatic potentials indicates a good fitting, its quality being slightly lower when the distance to the inner layer decreases.

The dependence between the electrostatic charges and the dipoles computed for formamide with respect to the number of points is reported in Table II. This study was performed considering four layers, the distance from the inner layer to the molecule being 1.4 times the van der Waals radii of the atoms. Calculations were carried out defining 50, 100, 200, 300, 400, and 1000 points. Charges, dipoles and relative RMS deviations shown in Table II exhibit a high degree of similarity, specially when the fitting is performed with more than 100 points.

Finally, Table III reports the influence of the number of layers on the electrostatic charges and the dipoles for formamide. Computations were carried out considering 200 points and locating the inner layer at 1.4 times the van der Waals radii of the atoms. A variable number of layers ranging from 1 to 6 was examined. As stated in Table III, very similar values of charges, dipoles and relative RMS deviations are obtained irrespective of the total number of layers, mainly when three or more layers are considered.

According to the preceding discussion, semiempirical electrostatic charges were derived by fitting the rigorous quantum chemical and the point-charge electrostatic potentials calculated in four layers, the inner layer being located at 1.4 times the van der Waals radii of the atoms and defining typically 200–300 points. These results agree with those reported by Singh and Kollman for the ab initio methodology to compute electrostatic charges.[14]

Electrostatic charges and dipoles of 21 selected molecules were calculated using electrostatic po-

Table I. MNDO and AM1 electrostatic charges and dipole for formamide as well as relative RMS deviations determined by fitting the rigorous quantum mechanical and the point-charge molecular electrostatic potentials calculated at 200 points located on four layers. The distance from the inner layer to the molecule is 1.2, 1.4, 1.6, and 1.8 times the van der Waals radii of the atoms.

Inner Layer	ATOM	Electrostatic Charges MNDO	Electrostatic Dipole MNDO	Relative RMS deviation MNDO	Electrostatic Charges AM1	Electrostatic Dipole AM1	Relative RMS deviation AM1
1.2	C	0.549	2.90	0.09	0.269	2.76	0.11
	O	-0.434			-0.311		
	N	-0.752			-0.730		
	H1	0.021			0.113		
	H2	0.321			0.333		
	H3	0.295			0.325		
1.4	C	0.517	2.92	0.06	0.202	2.75	0.08
	O	-0.425			-0.289		
	N	-0.738			-0.677		
	H1	0.034			0.132		
	H2	0.317			0.319		
	H3	0.294			0.313		
1.6	C	0.497	2.92	0.07	0.180	2.75	0.08
	O	-0.419			-0.280		
	N	-0.719			-0.653		
	H1	0.039			0.135		
	H2	0.313			0.309		
	H3	0.288			0.308		
1.8	C	0.489	2.92	0.06	0.157	2.75	0.07
	O	-0.416			-0.274		
	N	-0.705			-0.622		
	H1	0.040			0.140		
	H2	0.306			0.299		
	H3	0.285			0.299		

tentials evaluated from semiempirical (MNDO and AM1) and ab initio (STO-3G and 6-31G*) wavefunctions. Experimental as well as MNDO and AM1 optimized geometries were used in semiempirical computations, whereas ab initio calculations were performed from experimental geometries.[46] Results are shown in Tables IV (point charges) and V (dipoles), where Mulliken charges and dipoles as well as SCF dipoles derived from semiempirical calculations are also reported.

Relevance of Molecular Geometry in the Determination of Charges and Dipoles

Another interesting question to be examined lies in the dependence of the electrostatic potential-derived point charges and dipoles upon the molecular geometry used in semiempirical calculations. In this context, the work reported by Chirlian and Francl[11] clearly demonstrated the similarity of electrostatic charges obtained from experimental and ab initio 3-21G* optimized geometries, which led to the authors to recommend the use of such geometry to compute electrostatic charges when no experimental data are available. Nevertheless, the geometry optimization at the ab initio level for molecules, specially for compounds of biochemical and pharmacological interest, is very expensive. Consequently, the study of the reliability of the semiempirical optimized geometries to determine charges is of major importance.

Selected results of the comparison of both charges (Mulliken and electrostatic) and dipoles (computed from the Mulliken and the electrostatic charges as well as from the SCF charge distribution) obtained from computations performed with experimental and semiempirical optimized geometry are displayed in Table VI. Results clearly point out the extreme ability of the MNDO and AM1 optimized geometries for reproducing the charge distributions and the dipoles derived from experimental geometries. The inspection of Figure 1 also supports this conclusion. Accordingly, all the subsequent references in this work to semiempirical charges and dipoles will refer to the results derived from computations carried out using optimized geometries.

Reliability of Semiempirical Electrostatic Charges

The reliability of the Mulliken and electrostatic charges calculated from semiempirical wave functions to correctly reproduce the molecular charge distribution obtained from an ab initio computation was examined. For this purpose, the

Table II. MNDO and AM1 electrostatic charges and dipole for formamide as well as relative RMS deviations determined by fitting the rigorous quantum mechanical and the point-charge molecular electrostatic potentials calculated at 50, 100, 200, 300, 400, and 1000 points located on four layers. The distance from the inner layer to the molecule is 1.4 times the van der Waals radii of the atoms.

Number of Points	ATOM	Electrostatic Charges MNDO	Electrostatic Dipole MNDO	Relative RMS deviation MNDO	Electrostatic Charges AM1	Electrostatic Dipole AM1	Relative RMS deviation AM1
50	C	0.608	2.94	0.10	0.282	2.79	0.12
	O	-0.448			-0.308		
	N	-0.831			-0.741		
	H1	-0.004			0.092		
	H2	0.347			0.335		
	H3	0.325			0.340		
100	C	0.556	2.93	0.08	0.226	2.78	0.10
	O	-0.435			-0.296		
	N	-0.775			-0.687		
	H1	0.021			0.121		
	H2	0.325			0.317		
	H3	0.307			0.319		
200	C	0.517	2.92	0.07	0.202	2.75	0.09
	O	-0.425			-0.289		
	N	-0.737			-0.677		
	H1	0.034			0.132		
	H2	0.317			0.319		
	H3	0.294			0.313		
300	C	0.526	2.92	0.07	0 215	2.76	0.09
	O	-0.425			-0.292		
	N	-0.759			-0.692		
	H1	0.033			0.127		
	H2	0.323			0.322		
	H3	0.303			0.320		
400	C	0.538	2.92	0.07	0.222	2.76	0.09
	O	-0.430			-0.294		
	N	-0.757			-0.696		
	H1	0.027			0.125		
	H2	0.322			0.322		
	H3	0.299			0.320		
1000	C	0.521	2.92	0.07	0.205	2.76	0.09
	O	-0.426			-0.290		
	N	-0.738			-0.669		
	H1	0.032			0.128		
	H2	0.316			0.313		
	H3	0.295			0.312		

electrostatic potential-derived point-charges computed from the MNDO and AM1 semiempirical and the ab initio 6-31G* wave functions were compared (Table VII). This comparison also included the dipoles determined from such electrostatic charges, as well as those derived from Mulliken charges and from the SCF charge distribution.

Results shown in Table VII clearly state that the MNDO electrostatic charges reflect more precisely the 6-31G* electrostatic charge distribution than the Mulliken charges. Thus, the MNDO electrostatic charges explain up to the 96% of the variance of the 6-31G* electrostatic charges, while only the 77% of such variance is explained by the MNDO charges computed from the Mulliken population analysis (Fig. 2). Moreover, the regression coefficients (c) as well as the RMS deviations point out that the absolute values of the MNDO electrostatic charges are notably closer to the 6-31G* ones than the Mulliken charges.

The analysis of the dipoles supports these conclusions. When comparing the dipoles computed from the Mulliken charges, such MNDO dipoles exhibit a large difference in magnitude with respect to the ab initio 6-31G* ones, the regression equation explaining only the 74% of variance. On the other hand, the MNDO and the ab initio 6-31G* dipoles derived from the electrostatic charges are highly correlated (the 87% of the variance is explained by the regression equa-

Table III. MNDO and AM1 electrostatic charges and dipole for formamide as well as relative RMS deviations determined by fitting the rigorous quantum mechanical and the point-charge molecular electrostatic potentials calculated at 200 points located on a variable number (from 1 to 6) of layers. Results obtained from the fitting of 1000 points on six layers is also included for comparison purposes. The distance of the inner layer from the molecule is 1.4 times the van der Waals radii of the atoms.

Number of Layers	ATOM	Electrostatic Charges MNDO	Electrostatic Dipole MNDO	Relative RMS deviation MNDO	Electrostatic Charges AM1	Electrostatic Dipole AM1	Relative RMS deviation AM1
1	C	0.538	2.92	0.09	0.230	2.78	0.12
	O	-0.431			-0.298		
	N	-0.746			-0.694		
	H1	0.026			0.123		
	H2	0.317			0.320		
	H3	0.296			0.319		
2	C	0.555	2.91	0.08	0.241	2.76	0.10
	O	-0.434			-0.299		
	N	-0.779			-0.722		
	H1	0.023			0.121		
	H2	0.328			0.330		
	H3	0.307			0.328		
3	C	0.537	2.92	0.08	0.205	2.77	0.10
	O	-0.429			-0.289		
	N	-0.762			-0.691		
	H1	0.029			0.131		
	H2	0.322			0.323		
	H3	0.302			0.320		
4	C	0.517	2.92	0.08	0.202	2.75	0.09
	O	-0.425			-0.289		
	N	-0.738			-0.677		
	H1	0.034			0.132		
	H2	0.317			0.319		
	H3	0.294			0.313		
5	C	0.521	2.92	0.07	0.196	2.76	0.09
	O	-0.426			-0.287		
	N	-0.737			-0.655		
	H1	0.032			0.130		
	H2	0.316			0.309		
	H3	0.294			0.307		
6	C	0.537	2.93	0.07	0.218	2.76	0.09
	O	-0.430			-0.293		
	N	-0.754			-0.679		
	H1	0.028			0.124		
	H2	0.319			0.315		
	H3	0.300			0.316		
6 (1000 points)	C	0.530	2.92	0.07	0.203	2.76	0.09
	O	-0.427			-0.287		
	N	-0.751			-0.683		
	H1	0.030			0.130		
	H2	0.319			0.318		
	H3	0.300			0.318		

tion), their absolute values being more similar. It must be stressed that the ability of the MNDO electrostatic dipoles to correlate with the 6-31G* is almost identical to that exhibited by the MNDO SCF dipole. This fact is not surprising when looking at Figure 3, where it is clear that the MNDO electrostatic dipole highly correlates with the MNDO SCF dipole (r = 0.97), while a poor correlation (r = 0.86) is obtained with Mulliken charges-derived dipoles.

The AM1 results present some discrepancies with regard to the MNDO electrostatic charges and dipoles. Thus, although the nonconstant regression coefficient (c) and the RMS deviation obtained between the AM1 and the ab initio 6-31G* electrostatic charges are smaller than those derived from the comparison of the Mulliken charges (Table VII), the correlation coefficients in both cases are similar (Table VII, Fig. 4). At this respect, it should be noted

Table IV. Electrostatic and Mulliken charges of 21 selected molecules determined at the experimental and optimized geometries computed using MNDO and AM1 semiempirical methods and electrostatic charges at the experimental geometry computed using ab initio STO-3G and 6-31G* wave functions.[46] The numbering of the molecules is as follows.

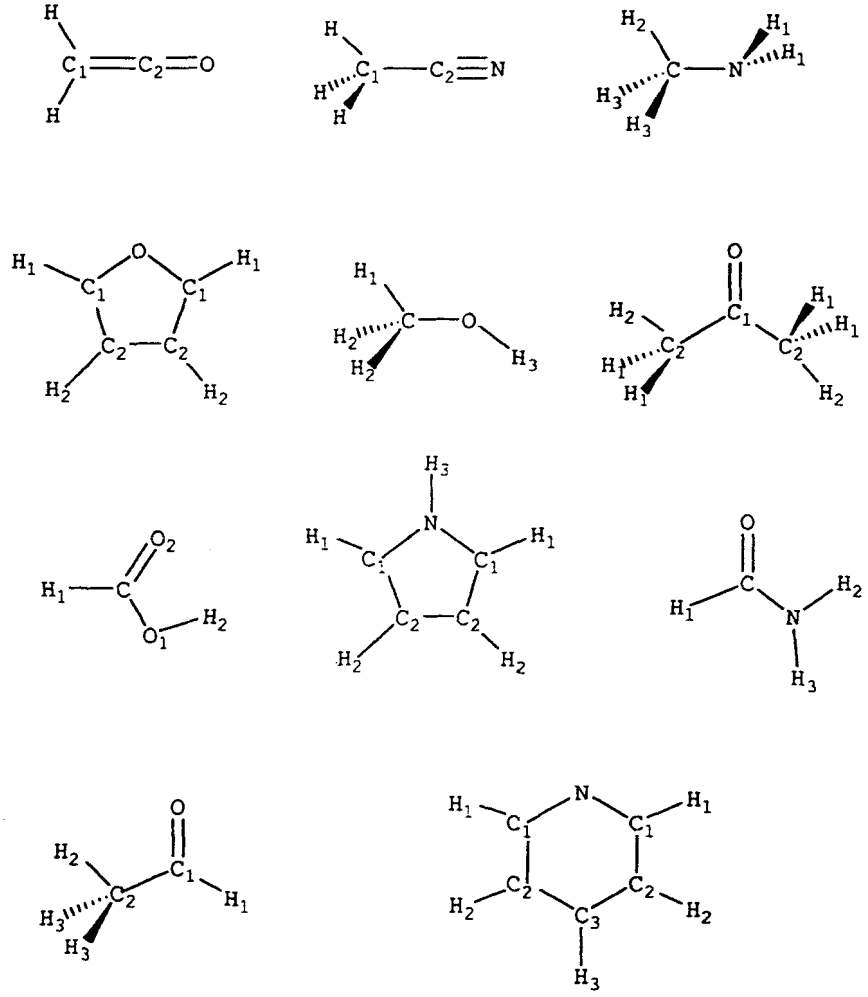

Molecule	Atom	MNDO				AM1				Electrost STO-3G exp geom	Electrost 6-31G* exp geom
		Experimental geometry		Optimized geometry		Experimental geometry		Optimized geometry			
		Mulliken	Electrostatic	Mulliken	Electrostatic	Mulliken	Electrostatic	Mulliken	Electrostatic		
HF	F	-0.284	-0.442	-0.287	-0.437	-0.280	-0.325	-0.289	-0.344	-0.298	-0.464
	H	0.284	0.442	0.287	0.437	0.280	0.325	0.289	0.344	0.298	0.464
CH4	C	0.072	-0.279	0.070	-0.296	-0.263	-0.562	-0.268	-0.595	-0.463	-0.490
	H	-0.018	0.070	-0.018	0.074	0.066	0.141	0.066	0.149	0.110	0.123
C2H4	C	-0.084	-0.229	-0.080	-0.214	-0.220	-0.348	-0.218	-0.345	-0.159	-0.343
	H	0.042	0.114	0.040	0.107	0.110	0.174	0.109	0.173	0.080	0.172
C2H2	C	-0.157	-0.264	-0.155	-0.261	-0.219	-0.342	-0.218	-0.340	-0.180	-0.295
	H	0.157	0.264	0.155	0.261	0.219	0.342	0.218	0.340	0.180	0.295
NH3	N	-0.245	-0.717	-0.226	-0.680	-0.362	-0.749	-0.396	-0.815	-0.953	-1.043
	H	0.082	0.239	0.075	0.227	0.121	0.250	0.132	0.272	0.318	0.348
CO2	C	0.447	0.670	0.448	-0.673	0.410	0.299	0.411	0.312	0.808	0.908
	O	-0.223	-0.335	-0.224	0.337	-0.205	-0.149	-0.206	-0.156	-0.404	-0.454
H2O	O	-0.318	-0.557	-0.326	-0.572	-0.385	-0.461	-0.383	-0.459	-0.615	-0.812
	H	0.159	0.278	0.163	0.286	0.192	0.231	0.191	0.230	0.308	0.406
CH2O	C	0.288	0.375	0.292	0.384	0.143	0.093	0.139	0.090	0.549	0.578
	O	-0.291	-0.351	-0.290	-0.355	-0.271	-0.235	-0.276	-0.244	-0.344	-0.503
	H	0.001	-0.012	-0.001	-0.015	0.064	0.071	0.069	0.077	-0.102	-0.037
COF2	C	0.620	0.974	0.605	0.956	0.501	0.335	0.480	0.313	0.880	0.950
	O	-0.262	-0.415	-0.275	-0.426	-0.270	-0.222	-0.279	-0.237	-0.443	-0.513
	F	-0.179	-0.279	-0.165	-0.265	-0.115	-0.057	-0.100	-0.038	-0.218	-0.219
HCN	C	-0.090	-0.079	-0.090	-0.078	-0.190	-0.263	-0.193	-0.265	0.207	0.107
	N	-0.100	-0.183	-0.100	-0.183	-0.048	-0.074	-0.048	-0.074	-0.323	-0.352
	H	0.191	0.261	0.190	0.261	0.236	0.337	0.239	0.339	0.116	0.245

Table IV. Continued

Molecule	Atom	MNDO				AM1				Electrost STO-3G exp geom	Electrost 6-31G* exp geom
		Experimental geometry		Optimized geometry		Experimental geometry		Optimized geometry			
		Mulliken	Electrostatic	Mulliken	Electrostatic	Mulliken	Electrostatic	Mulliken	Electrostatic		
CH2CO	C1	-0.289	-0.777	-0.277	-0.760	-0.452	-0.912	-0.441	-0.879	-0.768	-1.079
	C2	0.265	0.535	0.264	0.544	0.255	0.360	0.256	0.361	0.652	0.775
	O	-0.160	-0.266	-0.171	-0.280	-0.149	-0.134	-0.167	-0.155	-0.315	-0.412
	H	0.092	0.254	0.092	0.248	0.173	0.343	0.176	0.336	0.216	0.358
CH3CN	C1	0.136	-0.228	0.132	-0.228	-0.127	-0.411	-0.136	-0.433	-0.497	-0.390
	C2	-0.118	0.131	-0.115	0.136	-0.148	0.027	-0.145	0.037	0.475	0.433
	N	-0.081	-0.219	-0.080	-0.218	-0.050	-0.145	-0.050	-0.147	-0.448	-0.503
	H	0.021	0.105	0.021	0.103	0.108	0.177	0.110	0.181	0.156	0.153
CH3NH2	N	-0.317	-0.737	-0.306	-0.719	-0.355	-0.714	-0.346	-0.697	-0.860	-1.059
	C	0.141	0.225	0.131	0.192	-0.123	-0.001	-0.130	-0.038	0.289	0.424
	H1	0.104	0.272	0.104	0.271	0.140	0.282	0.141	0.282	0.315	0.384
	H2	-0.043	-0.048	-0.042	-0.040	0.031	0.006	0.026	0.009	-0.029	-0.086
	H3	0.005	0.007	0.005	0.012	0.083	0.072	0.084	0.081	-0.015	-0.023
FURAN	O	-0.158	-0.134	-0.126	-0.113	-0.107	0.031	-0.107	0.018	-0.182	-0.200
	C1	0.007	-0.079	-0.012	-0.075	-0.092	-0.261	-0.097	-0.246	0.051	-0.064
	C2	-0.135	-0.191	-0.132	-0.205	-0.205	-0.255	-0.199	-0.263	-0.108	-0.180
	H1	0.123	0.193	0.118	0.178	0.196	0.286	0.189	0.270	0.082	0.191
	H2	0.085	0.144	0.090	0.159	0.155	0.216	0.161	0.230	0.066	0.153
CH3OH	O	-0.328	-0.468	-0.329	-0.477	-0.330	-0.329	-0.326	-0.317	-0.470	-0.638
	C	0.188	0.143	0.194	0.162	-0.065	-0.254	-0.072	-0.302	0.141	0.189
	H1	0.018	0.044	0.018	0.040	0.098	0.160	0.101	0.172	0.020	0.052
	H2	-0.024	-0.009	-0.031	-0.019	0.050	0.084	0.051	0.095	0.002	-0.002
	H3	0.171	0.299	0.180	0.312	0.196	0.255	0.196	0.256	0.304	0.401
CO(CH3)2	O	-0.286	-0.383	-0.290	-0.386	-0.291	-0.297	-0.300	-0.311	-0.400	-0.590
	C1	0.199	0.586	0.195	0.581	0.231	0.467	0.226	0.494	0.713	0.796
	C2	-0.008	-0.507	-0.003	-0.505	-0.267	-0.649	-0.269	-0.682	-0.555	-0.512
	H1	0.005	0.129	0.006	0.128	0.085	0.186	0.086	0.194	0.127	0.117
	H2	0.023	0.138	0.022	0.140	0.106	0.189	0.110	0.199	0.136	0.146
FORMIC ACID	O1	-0.276	-0.488	-0.313	-0.538	-0.300	-0.334	-0.325	-0.357	-0.531	-0.646
	O2	-0.355	-0.462	-0.369	-0.472	-0.343	-0.312	-0.357	-0.326	-0.403	-0.554
	C	0.349	0.564	0.360	0.567	0.263	0.177	0.260	0.151	0.597	0.630
	H1	0.081	0.047	0.106	0.080	0.148	0.178	0.179	0.229	-0.021	0.092
	H2	0.202	0.338	0.216	0.363	0.232	0.292	0.242	0.303	0.358	0.478
PIRROL	N	-0.198	-0.151	-0.224	-0.225	-0.170	-0.100	-0.186	-0.138	-0.117	-0.238
	C1	-0.041	-0.233	-0.028	-0.178	-0.149	-0.338	-0.144	-0.322	-0.115	-0.203
	C2	-0.127	-0.162	-0.129	-0.188	-0.194	-0.227	-0.196	-0.235	-0.111	-0.196
	H1	0.085	0.180	0.092	0.181	0.155	0.245	0.160	0.250	0.092	0.182
	H2	0.079	0.144	0.077	0.150	0.149	0.211	0.151	0.215	0.073	0.164
	H3	0.207	0.292	0.199	0.296	0.246	0.318	0.247	0.324	0.238	0.344
NH2COH	C	0.389	0.517	0.375	0.491	0.281	0.202	0.257	0.176	0.523	0.664
	O	-0.355	-0.425	-0.371	-0.436	-0.341	-0.289	-0.371	-0.323	-0.404	-0.580
	N	-0.433	-0.738	-0.430	-0.732	-0.474	-0.677	-0.448	-0.646	-0.697	-0.931
	H1	0.036	0.034	0.056	0.063	0.099	0.132	0.119	0.159	-0.026	0.016
	H2	0.184	0.317	0.189	0.322	0.217	0.319	0.223	0.322	0.295	0.405
	H3	0.179	0.294	0.180	0.293	0.218	0.313	0.219	0.312	0.307	0.426
CH3COH	C1	0.241	0.409	0.242	0.407	0.185	0.213	0.182	0.214	0.500	0.586
	O	-0.289	-0.362	-0.288	-0.362	-0.285	-0.265	-0.290	-0.274	-0.342	-0.527
	C2	-0.022	-0.291	-0.025	-0.293	-0.283	-0.417	-0.288	-0.432	-0.454	-0.393
	H1	0.012	-0.007	0.014	-0.004	0.080	0.067	0.085	0.074	-0.059	-0.019
	H2	0.008	0.066	0.008	0.068	0.087	0.120	0.089	0.125	0.099	0.086
	H3	0.024	0.092	0.024	0.091	0.107	0.141	0.114	0.147	0.128	0.134
PYRIDINE	N	-0.220	-0.476	-0.221	-0.472	-0.136	-0.343	-0.137	-0.341	-0.643	-0.676
	C1	0.052	0.289	0.049	0.277	-0.070	0.137	-0.074	0.126	0.512	0.467
	C2	-0.123	-0.396	-0.123	-0.385	-0.181	-0.430	-0.181	-0.426	-0.430	-0.549
	C3	-0.006	0.131	-0.007	0.114	-0.090	0.047	-0.093	0.037	0.300	0.308
	H1	0.079	0.073	0.082	0.079	0.155	0.147	0.158	0.154	-0.039	0.043
	H2	0.072	0.161	0.072	0.159	0.141	0.217	0.143	0.220	0.123	0.201
	H3	0.066	0.091	0.067	0.098	0.136	0.153	0.138	0.158	0.010	0.044

(see Table IV) the large differences between the electrostatic charges and those derived from Mulliken population analysis for the MNDO method, the same wide variation being reported for ab initio methods,[10,11,14] but in contrast both types of charge distributions exhibit a strong similarity for the AM1 results in numerous cases.

AM1 electrostatic dipoles are very similar to the MNDO ones and reflect correctly the dipoles computed from the 6-31G* electrostatic charges (r = 0.94) and from the AM1 SCF charge distribution (r = 0.96) (Fig. 5). Results displayed in Table VII also point out that the dipoles derived from the AM1 electrostatic charges reproduce the ab initio 6-31G* electrostatic dipoles better than the AM1 dipoles determined from the Mulliken charges.

Comparison of the Ability of the Different Charge Distributions to Reproduce Experimental Dipole Moments

The ability of MNDO and AM1 dipoles computed from Mulliken population analysis, electrostatic charges and from the SCF calculations to reproduce experimental dipole moments was examined and compared with that of ab initio STO-3G and 6-31G* electrostatic charges-derived dipoles.

Table V. Mulliken, SCF and electrostatic dipoles of 21 selected molecules determined at the experimental and optimized geometries computed using MNDO and AM1 semiempirical methods and electrostatic dipoles at the experimental geometry computed using the ab initio STO-3G and 6-31G* wave functions.[46]

MOLECULE	MNDO						AM1								
	Experimental geometry			Optimized geometry			Experimental geometry			Optimized geometry			Electrost STO-3G exp geom	Electrost 6-31G* exp geom	Experimental
	Mulliken	SCF	Electrostatic	Mulliken	SCF	Electrostatic	Mulliken	SCF	Electrostatic	Mulliken	SCF	Electrostatic			
HF	1.25	1.95	1.95	1.32	2.00	2.01	1.23	1.76	1.43	1.15	1.74	1.36	1.31	2.04	1.82
NH3	0.45	1.74	1.31	0.44	1.75	1.31	0.66	1.93	1.37	0.64	1.85	1.33	1.74	1.91	1.47
H2O	0.90	1.79	1.57	0.88	1.78	1.55	1.08	1.85	1.30	1.09	1.86	1.31	1.75	2.29	1.85
CH2O	1.69	2.15	1.97	1.69	2.16	1.99	1.93	2.23	1.76	2.02	2.32	1.87	1.42	2.71	2.33
CP2O	0.15	0.49	0.27	0.44	0.81	0.61	0.67	1.02	0.83	0.91	1.28	1.12	0.88	1.27	0.95
HCN	1.53	2.51	2.35	1.52	2.50	2.35	1.46	2.35	2.13	1.48	2.36	2.16	2.39	3.20	2.98
CH2CO	0.70	0.82	1.05	0.89	1.04	1.28	1.03	0.97	1.03	1.37	1.35	1.44	0.68	1.80	1.42
CH3CN	1.96	2.65	2.39	1.92	2.63	2.37	2.24	2.88	2.57	2.24	2.89	2.59	3.14	4.10	3.92
CH3NH2	0.40	1.44	1.00	0.35	1.42	1.00	0.55	1.58	1.00	0.48	1.55	0.95	1.40	1.48	1.31
FURAN	0.02	0.27	0.09	0.16	0.42	0.33	0.02	0.22	0.32	0.35	0.49	0.10	0.25	0.66	0.66
CH3OH	0.93	1.58	1.27	0.79	1.47	1.17	1.15	1.65	1.00	1.13	1.62	0.99	1.44	1.83	1.70
CO(CH3)2	1.96	2.41	2.20	2.01	2.44	2.22	2.34	2.69	2.17	2.46	2.78	2.28	1.87	3.24	2.88
FORMIC ACID	1.43	1.28	1.29	1.66	1.49	1.52	1.50	1.29	1.32	1.76	1.48	1.61	0.74	1.52	1.41
PIRROL	1.36	1.94	1.76	1.25	1.81	1.66	1.47	2.06	1.88	1.36	1.97	1.76	1.90	1.89	1.74
NH2COH	2.41	3.19	2.92	2.62	3.36	3.11	2.71	3.32	2.76	3.11	3.70	3.17	2.86	4.32	3.73
CH3COH	1.86	2.34	2.10	1.87	2.34	2.12	2.19	2.52	2.01	2.28	2.60	2.12	1.73	3.09	2.69
PYRIDINE	0.91	1.98	1.54	0.93	1.99	1.58	0.91	1.98	1.35	0.93	1.98	1.36	2.05	2.21	2.22

Table VI. Statistical parameters of the comparison between electrostatic charges and dipoles, Mulliken charges and dipoles and SCF dipoles calculated by using MNDO and AM1 methods at the experimental and optimized geometries. Variables x and y refer to charges or dipoles determined using optimized and experimental geometries, respectively.

	MNDO			AM1		
	y= ax + b	y = cx	RMS deviation	y= ax + b	y = cx	RMS deviation
Mulliken Charges	a= 0.99 b= 0.00 r= 0.99	c= 0.99 r= 0.99	0.01	a= 0.99 b= 0.00 r= 0.99	c= 0.99 r= 0.99	0.01
Electrostatic Charges	a= 1.00 b= 0.00 r= 0.99	c= 1.00 r= 0.99	0.04	a= 0.98 b= 0.00 r= 0.99	c= 0.98 r= 0.99	0.02
Mulliken Dipole	a= 0.99 b= -0.03 r= 0.98	c= 0.97 r= 0.98	0.17	a= 0.94 b= -0.01 r= 0.98	c= 0.93 r= 0.98	0.18
Electrostatic Dipole	a= 1.05 b= -0.16 r= 0.98	c= 0.97 r= 0.98	0.15	a= 1.01 b= -0.11 r= 0.98	c= 0.94 r= 0.97	0.19
SCF Dipole	a= 1.06 b= -0.15 r= 0.99	c= 0.98 r= 0.99	0.13	a= 0.88 b= 0.13 r= 0.97	c= 0.96 r= 0.98	0.17

Statistical parameters of this study are shown in Table VIII.

The dipoles determined from semiempirical SCF charge distributions reproduce correctly the experimental dipole moments in agreement with previous works.[33,40,42] MNDO and AM1 dipoles derived from electrostatic charges clearly correlate with experimental values, the statistical parameters being similar for both methods. Dipoles obtained from Mulliken charges show the poorest agreement with the experimental dipoles. These results are not surprising, since both MNDO and AM1 methods were parametrized to reproduce experimental dipole moments and the electrostatic charge distribution leads to dipoles in close agreement with those determined from the SCF calculation.

On the other hand, dipoles computed from the 6-31G* electrostatic charges correlate almost perfectly with the experimental values, the experimental dipole moment being underestimated by a factor of 0.89, whereas a correlation of smaller quality is obtaining when dealing with the dipoles determined from the STO-3G electro-

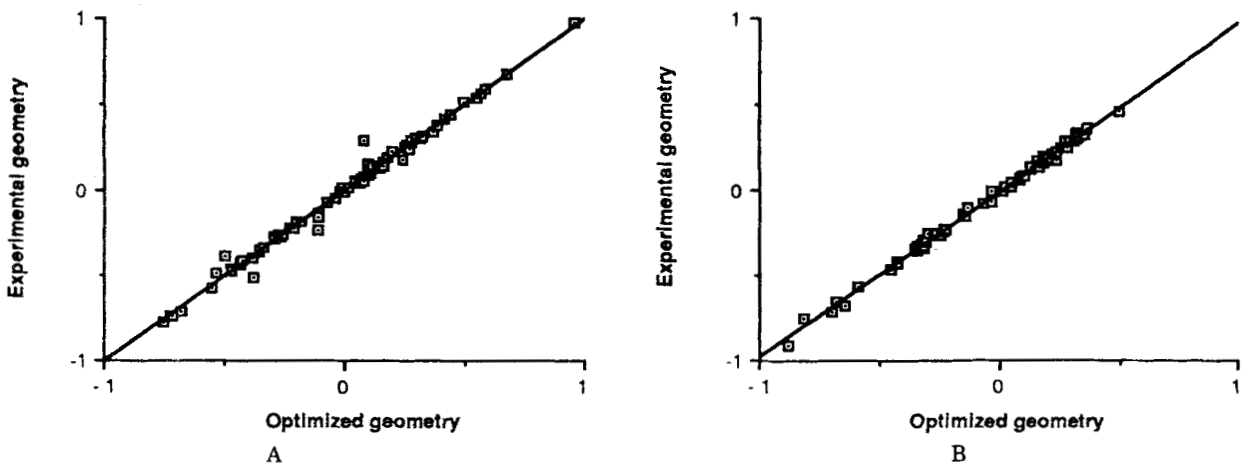

Figure 1. Plot of the relationship existing between the electrostatic charges determined from optimized (x) and experimental (y) geometries using (A) MNDO and (B) AM1 methods.

Table VII. Statistical parameters of the comparison between electrostatic charges and dipoles, Mulliken charges and dipoles and SCF dipoles calculated by using MNDO and AM1 methods and the ab initio 6-31G* electrostatic charges and dipoles. Variables x and y refer to the different electrostatic charges or dipoles computed using the semiempirical and the ab initio 6-31G* wave functions, respectively.

	MNDO			AM1		
	y= ax + b	y = cx	RMS deviation	y= ax + b	y = cx	RMS deviation
Mulliken Charges	a= 2.03 b= -0.02 r= 0.88	c= 2.03 r= 0.88	0.30	a= 1.86 b= 0.01 r= 0.88	c= 1.86 r= 0.88	0.29
Electrostatic Charges	a= 1.32 b= -0.01 r= 0.98	c= 1.32 r= 0.98	0.14	a= 1.30 b= 0.01 r= 0.88	c= 1.30 r= 0.88	0.24
Mulliken Dipole	a= 1.23 b= 0.82 r= 0.86	c= 1.75 r= 0.75	1.22	a= 1.11 b= 0.71 r= 0.85	c= 1.50 r= 0.78	1.01
Electrostatic Dipole	a= 1.33 b= 0.12 r= 0.93	c= 1.39 r= 0.93	0.79	a= 1.30 b= 0.21 r= 0.94	c= 1.41 r= 0.93	0.81
SCF Dipole	a= 1.30 b= -0.07 r= 0.94	c= 1.26 r= 0.94	0.61	a= 1.28 b= -0.23 r= 0.96	c= 1.18 r= 0.96	0.48

static charges, this basis set leading to slightly worse results than the semiempirical methods.

On the Scaling of Semiempirical Charge Distributions

The analysis of the charge distributions derived from ab initio wave functions of different quality led to propose the correction of the charge distribution originated from a low quality wave function by means of a scaling factor in order to reproduce charges derived from a more sophisticated wave function.[10,11] Particularly, Chirlian and Francl[11] used a regression equation of the type $y = ax + b$ for scaling the 3-21G electrostatic charges to the 6-31G* ones. Nevertheless, the use of a regression equation of the type $y = cx$ seems to be more adequate, since then both the dipole and the charges are corrected by the same constant c and the goodness of the scaling can be easily tested.

Scaling factors for MNDO and AM1 methods were determined by comparing the semiempirical and the ab initio 6-31G* electrostatic charges.

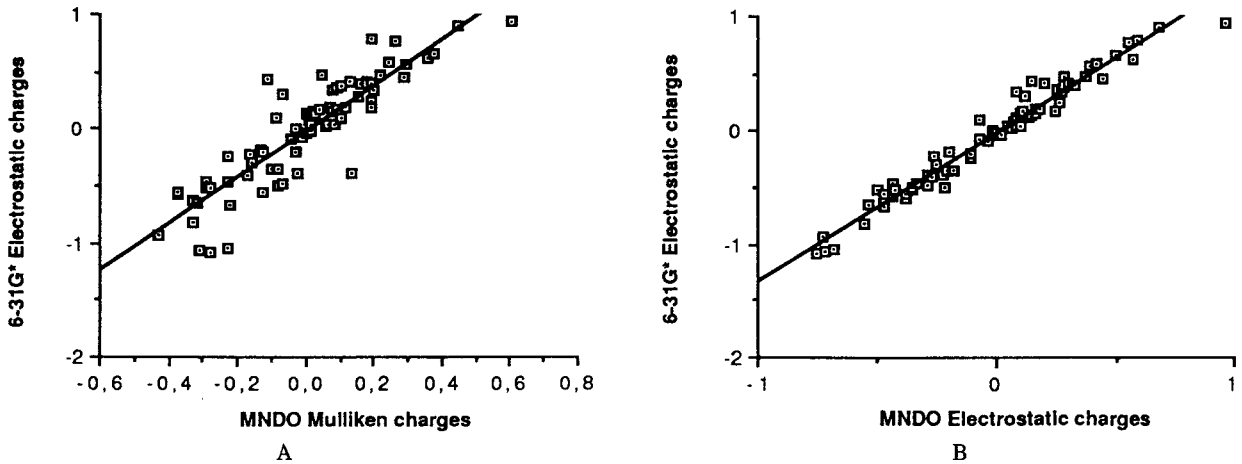

Figure 2. Plot of the relationship existing between (A) Mulliken and (B) electrostatic charges computed using the MNDO with respect to the ab initio 6-31G* electrostatic charges.

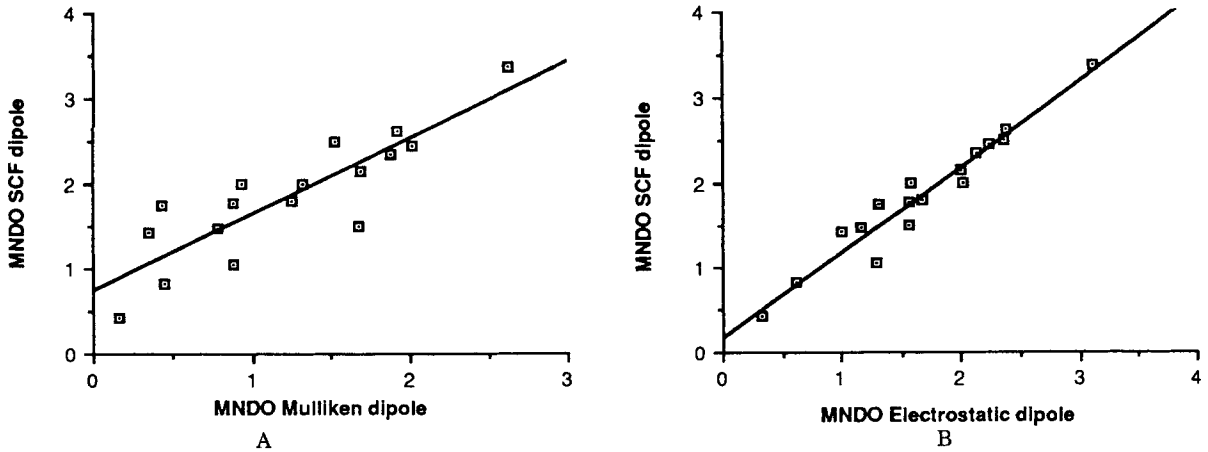

Figure 3. Plot of the relationship existing between (A) Mulliken and (B) electrostatic dipoles computed using the MNDO with respect to the SCF dipoles determined from MNDO computations.

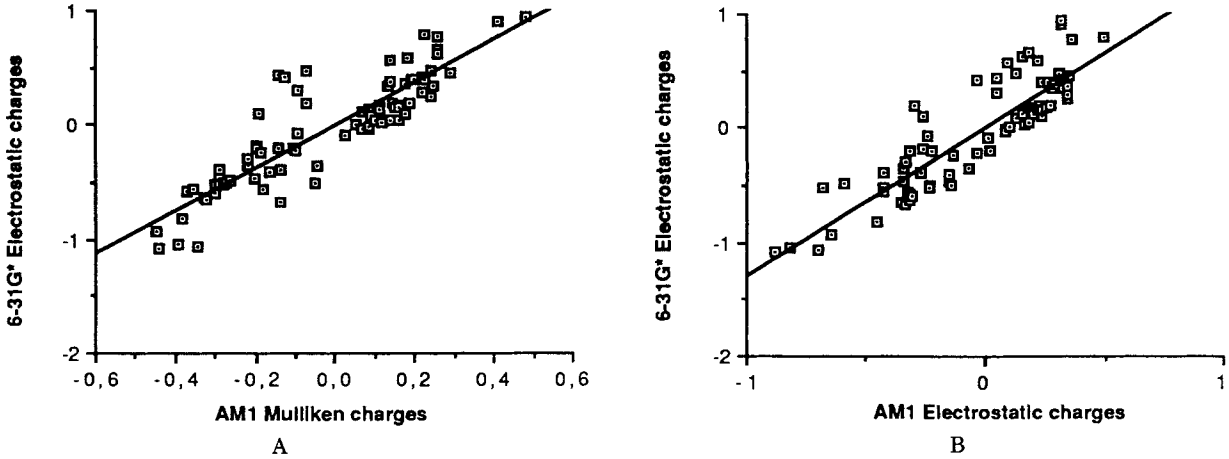

Figure 4. Plot of the relationship existing between (A) Mulliken and (B) electrostatic charges computed using the AM1 method with respect to the ab initio 6-31G* electrostatic charges.

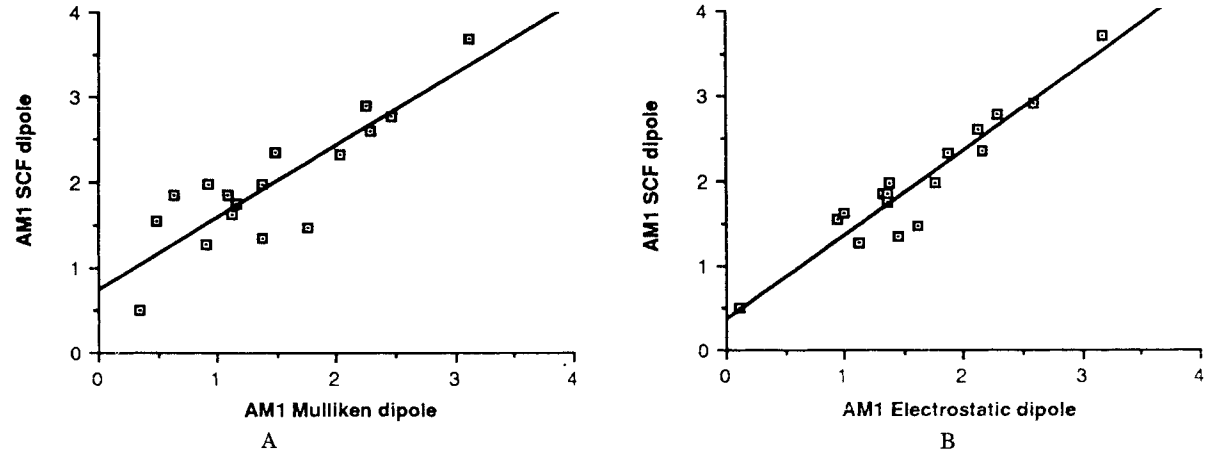

Figure 5. Plot of the relationship existing between (A) Mulliken and (B) electrostatic dipoles computed using the AM1 method with respect to the SCF dipoles determined from AM1 computations.

The values of such scaling factors for MNDO and AM1 electrostatic charges are 1.32 and 1.30, respectively. The scaling factors of the semiempirical charges-derived dipoles with regard to the 6-31G* ones are 1.39 and 1.41 for MNDO and AM1, respectively. From a theoretical viewpoint, the scaling factors of charges and dipoles for each semiempirical method should be identical, and in practice they are very similar, specially for the MNDO method. The discrepancies can be

Table VIII. Statistical parameters of the comparison between the Mulliken, SCF and electrostatic dipoles calculated by using MNDO and AM1 methods, ab initio STO-3G and 6-31G* methods and the electrostatic dipoles determined by the scaled MNDO and AM1 electrostatic charges with respect to the gas phase experimental dipoles. Variables x and y refer to the theoretical and experimental dipole moments.

		MULLIKEN DIPOLE	ELECTROSTATIC DIPOLE	SCF DIPOLE
MNDO	y= ax+b	a= 1.13 b= 0.68 r= 0.85	a= 1.22 b= 0.05 r= 0.92	a= 1.19 b= -0.14 r= 0.93
	y =cx	c= 1.56 r= 0.77	c= 1.24 r= 0.92	c= 1.12 r= 0.93
	RMS deviation	0.97	0.56	0.41
AM1	y= ax+b	a= 0.99 b= 0.61 r= 0.82	a= 1.18 b= 0.15 r= 0.91	a= 1.16 b= -0.25 r= 0.94
	y =cx	c= 1.33 r= 0.77	c= 1.26 r= 0.91	c= 1.05 r= 0.93
	RMS deviation	0.79	0.58	0.37
STO-3G	y= ax+b		a= 1.09 b= 0.30 r= 0.89	
	y =cx		c= 1.24 r= 0.88	
	RMS deviation		0.60	
6-31G*	y= ax+b		a= 0.92 b= -0.07 r= 0.99	
	y =cx		c= 0.89 r= 0.99	
	RMS deviation		0.31	
Corrected MNDO	y= ax+b		a= 0.93 b= 0.05 r= 0.92	
	y =cx		c= 0.94 r= 0.92	
	RMS deviation		0.38	
Corrected AM1	y= ax+b		a= 0.91 b= 0.16 r= 0.91	
	y =cx		c= 0.97 r= 0.91	
	RMS deviation		0.38	

attributed to (1) the fact that the fit of the regression equations is not perfect, specially for the AM1 electrostatic charges, and (2) that the charge scaling factors were obtained from 81 points, while the dipole ones were determined from 17 points only.

The corrected MNDO and AM1 charges calculated by means of the corresponding charge scaling factors reproduce more precisely both electrostatic charges and dipoles determined at the 6-31G* level, as stated by comparing the RMS deviations between the 6-31G* electrostatic

charges and the semiempirical ones before and after the scaling procedure: RMS (MNDO—6-31G*) = 0.14, RMS (corrected MNDO—6-31G*) = 0.09); RMS (AM1—6-31G*) = 0.24, RMS (corrected AM1—6-31G*) = 0.22. The improvement due to the scaling of electrostatic charges for MNDO is greater than for AM1, as it could be expected.

The scaling of the electrostatic charges also improves the representation of the 6-31G* electrostatic charges-derived dipoles when dealing with those computed from the corrected semiempirical charges: RMS (MNDO—6-31G*) = 0.79, RMS (corrected MNDO—6-31G*) = 0.38); RMS (AM1—6-31G*) = 0.81, RMS (corrected AM1—6-31G*) = 0.40.

Finally, results displayed in Table VIII clearly demonstrate the great coincidence between the experimental dipoles and the corrected semiempirical electrostatic charges-derived dipoles. Note the small value of the RMS deviation, which is very similar to that obtained from the 6-31G* electrostatic dipoles and largely better than that obtained from the STO-3G ones, as well as the value very close to unity of the regression coefficient c.

CONCLUSIONS

In agreement with the suggestions proposed by Singh and Kollman for the ab initio electrostatic charges,[14] the computation of reliable electrostatic charges determined by fitting the molecular electrostatic potential evaluated from the semiempirical MNDO and AM1 wavefunctions[23] should require the calculation of the electrostatic potential at 200–300 points placed on four layers, the inner layer being located at 1.4 times the van der Waals radii of the atoms.

The strong similarity of the electrostatic charges and the dipoles obtained from computations carried out using either the experimental or the semiempirical optimized geometry permit to recommend the semiempirical optimized geometry to evaluate the electrostatic potential-derived charges and dipoles when no experimental data are available.

Results presented in this article reveal the usefulness of semiempirical wave functions to compute electrostatic charges at a low computational cost. MNDO electrostatic charges have proved their great ability to reproduce the sophisticated ab initio 6-31G*, the AM1 electrostatic charges showing a smaller ability. Both semiempirical methods provide electrostatic charges-derived dipoles highly correlated with the semiempirical SCF, electrostatic 6-31G* and experimental dipoles. Indeed, a very accurate description of the 6-31G* electrostatic charge distributions can be obtained by applying an adequate scaling factor to the semiempirical electrostatic charges, specially when the MNDO method is used, the dipoles derived from such corrected charges having a close similarity to the experimentally determined dipole values, reinforcing the goodness of the method.

We are grateful to Dr. S. Olivella and Dr. J. M. Bofill for making available their version of MOPAC program and Dr. R. Cimiraglia for sending us a copy of the ab initio molecular electrostatic potential computation program, which was then modified to carry out the present study. We also thank the Centre de Calcul de la Universitat de Barcelona for computational facilities.

Note added in proof: When this paper was in press two related papers, one by Ferenczy et al. (J. Comput. Chem., **11**, 159-169 (1990)), and the other by Besler et al. (J. Comput. Chem., **11**, 431-439 (1990)) appeared. Besler, Merz and Kollman used a methodological approach very similar to that described here. Their results are very similar to ours, and point out the effectiveness of the semiempirical electrostatic charges, especially when the MNDO wavefunction is used. Ferenczy, Reynolds and Richards used a slightly different approach to that employed in this work, since they maintained in the calculation of the MEP some of the approximations used to compute the AM1 wavefunction. Results reported by this group are slightly different from those reported by Kollman's group and by ourselves, but the general behavior of the semiempirical charges is similar. The general accordance between the results obtained by three independent research groups strongly support the effectiveness of the semiempirical derived electrostatic charges.

References

1. K. Kitaura and K. Morokuma, *Int. J. Quantum Chem.*, **10**, 325 (1976).
2. J. Langlet, P. Claverie, F. Caron, and J. C. Boeuve, *Int. J. Quantum Chem.*, **19**, 299 (1981).
3. A. Pullman, C. Zakrewska, and D. Perahia, *Int. J. Quantum Chem.*, **16**, 393 (1979).
4. W. A. Sokalski and R. Poirier, *Chem. Phys. Lett.*, **98**, 86 (1983).
5. R. S. Mulliken, *J. Chem. Phys.*, **23**, 1833 (1955).
6. F. A. Momany, *J. Phys. Chem.*, **82**, 592 (1978).
7. R. J. Abraham and P. E. Smith, *J. Comp. Chem.*, **9**, 288 (1988).
8. J. Mullay, *J. Comp. Chem.*, **9**, 399 (1988).
9. J. J. Houser and G. Klopman, *J. Comp. Chem.*, **9**, 893 (1988).
10. S. R. Cox and D. E. Williams, *J. Comp. Chem.*, **2**, 304 (1981).
11. L. E. Chirlian and M. E. Fracl, *J. Comp. Chem.*, **8**, 894 (1987).
12. J. R. Rabinowitz and S. B. Little, *Int. J. Quantum Chem.: Quantum Chem. Symp.*, **22**, 721 (1988).
13. P. H. Smit, J. L. Derissen, and F. B. van Duijneveldt, *Mol. Phys.*, **37**, 521 (1979).
14. U. C. Singh and P. A. Kollman, *J. Comp. Chem.*, **5**, 129 (1984).

15. P.K. Weiner and P.A. Kollman, *J. Comp. Chem.*, **2,** 287 (1981).
16. S.J. Weiner, P.A. Kollman, D.A. Case, U.C. Singh, C. Ghio, G. Alagona, S. Profeta, Jr., and P. Weiner, *J. Am. Chem. Soc.*, **106,** 765 (1984).
17. S.J. Weiner, P.A. Kollman, D.T. Nguyen, and D.A. Case, *J. Comp. Chem.*, **7,** 230 (1986).
18. C. Giessner-Prettre and A. Pullman, *Theor. Chim. Acta,* **25,** 83 (1972).
19. C. Giessner-Prettre and A. Pullman, *Theor. Chim. Acta,* **33,** 91 (1974).
20. C. Giessner-Prettre and A. Pullman, *Theor. Chim. Acta,* **37,** 335 (1975).
21. J.C. Culberson and M.C. Zerner, *Chem. Phys. Lett.*, **122,** 436 (1985).
22. S. Srebrenick, H. Weinstein, and R. Pauncz, *Chem. Phys. Lett,* **20,** 419 (1973).
23. F.J. Luque, F. Illas, and M. Orozco, *J. Comp. Chem.*, **11,** 416-430 (1990).
24. J.A. Pople, D.P. Santry, and G.A. Segal, *J. Chem. Phys.*, **43,** S129 (1965).
25. J.A. Pople and G.A. Segal, *J. Chem. Phys.*, **43,** S136 (1965).
26. J.A. Pople, D.L. Beveridge, and P.A. Dobosh, *J. Chem. Phys.*, **47,** 2026 (1967).
27. C. Petrongolo, *Gazz. Chim. Ital.*, **108,** 445 (1978).
28. J.J. Kaufman, P.C. Hariharan and F.L. Tobin, in *Chemical Applications of Atomic and Molecular Electrostatic Potentials,* P. Politzer and D.G. Truhlar Eds., Plenum, New York, 1981, pp. 335–380.
29. G. Náray-Szabó and P.R. Surján, in *Theoretical Chemistry of Biological Systems,* G. Náray-Szabó, Ed., Elsevier, Amsterdam, 1986, pp. 1–100.
30. A.J. Duben, *Theor. Chim. Acta.*, **59,** 81 (1981).
31. M.J.S. Dewar and W. Thiel, *J. Am. Chem. Soc.*, **99,** 4899 (1977).
32. P.C. Hariharan and J.A. Pople, *Theor. Chim. Acta.*, **28,** 213 (1973).
33. M.J.S. Dewar, E.G. Zoebisch, E.F. Horsley, and J.J.P. Stewart, *J. Am. Chem. Soc.*, **107,** 3902 (1985).
34. W.J. Hehre, R.F. Stewart and J.A. Pople, *J. Chem. Phys.*, **51,** 2657 (1969).
35. E. Scrocco and J. Tomasi, *Topics in Curr. Chem.*, **42,** 381 (1973).
36. P.O. Löwdin, *J. Chem. Phys.*, **56,** 365 (1970).
37. W.H. Press, B.P. Flannery, S.A. Teukolsly, and W.T. Vettering, *Numerical Recipes,* Cambridge University Press, Cambridge, 1986.
38. S. Olivella, *QCPE Bull.*, **4,** 109 (1984). Modified by S. Olivella and J.M. Bofill, 1987.
39. J.J.P. Stewart, *QCPE Bull.*, **3,** 101 (1983).
40. M.J.S. Dewar and W. Thiel, *J. Am. Chem. Soc.*, **99,** 4907 (1977).
41. M.J.S. Dewar and E.G. Zoebisch, *J. Mol. Struc. (THEOCHEM),* **180,** 1 (1988).
42. J.J.P. Stewart, *J. Comp. Chem.*, **10,** 221 (1989).
43. M. Dupuis, J. Rys, and H.F. King, *QCPE Bull.*, **58,** 17 (1977).
44. M. Connolly, *QCPE Bull.*, **1,** 75 (1981).
45. The same study was performed for water molecule. The results, which are available upon request, exhibit identical trends that those reported for the formamide molecule.
46. The ab initio electrostatic charges and dipoles for HF, H_2O, NH_3, CH_4, C_2H_2, C_2H_4, CO_2, H_2CO, CH_3OH, H_2NCHO, HCOOH, CH_3CH and CH_2CO were taken from reference 11.